Computer Science and Information Systems 21(4):1801–1822 https://doi.org/10.2298/CSIS240418058W

Attitude Estimation of Aircraft Based on Quaternion SRCKF-SLAM Algorithm

Dandan Wang [1,2,*], Zhaokun Zhu[3], Liang Yu[1], Hongjie Li[4], and Kaituo Tan[1]

[1] School of Mechanical and Electrical Engineering, Huainan normal university, 232038 Huainan Anhui,P.R.China;
lansejingling1988@126.com
[2] Human-computer collaborative robot Joint Laboratory of Anhui Province, 232038 Huainan Anhui,P.R.China;
[3] School of Information Engineering, Zhengzhou Technology and Business University, 475000 Zhengzhou Henan,P.R.China;
[4] College of Electronic Information and Electrical Engineering, Anyang Institute Of Technology, 455000 Anyang Henan, P.R. China;

Abstract. In complex terrain environments such as high mountains and hills, traditional agricultural machinery cannot accurately complete tasks such as crop management and harvesting. This paper used plant protection drones as carriers to study the observation content of crops during their navigation process. Aiming at the low accuracy of the traditional quaternion cubature Kalman filtering algorithm for the attitude estimation of the carrier nonlinear state model, a quaternon-based square root cubature Kalman filtering algorithm was proposed in this paper.The algorithm takes the attitude quaternion error and the gyro drift error as the state quantity, and measures the attitude quaternion of SINS/SLAM navigation. The square root cubature Kalman filter algorithm is used for pose estimation, which not only solves the standardization problem of traditional quaternion, but also reduces the state dimension and complexity of the square root UKF algorithm of traditional quaternion, and improves the numerical stability. Compared with the quaternion SRUKF and quaternion SRCDKF algorithm, the simulation results showed that the new algorithm estimated the error mean values of the roll angle, pitch angle and runt angle, which are 0.05°, 0.08°, and 0.03°, respectively. The error is the smallest, and algorithm accuracy is about 30% higher than the quaternion SRUKF-SLAM algorithm, and it has high filtering accuracy and numerical stability, and the best time-consuming performanc.

Keywords: quaternion, state model, square root Cubature Kalman filter, attitude estimation, numerical stability.

1. Introduction

As a new star in smart agriculture, plant protection drones carry important tasks such as precise pesticide application, targeted fertilization, environmental monitoring, information collection and processing. The accuracy of drone tracking and pose

* Corresponding Author

estimation is the technical guarantee for achieving the detection and orderly management of crop growth environment[1-3].When dealing with non-linear state models in target tracking systems, attitude quaternions are usually used as the attitude model parameters of the carrier[4-6], which has the advantages of smaller global dimension and non-singularity than Euler angle attitude parameter description methods and can achieve target full attitude tracking.

Firstly, starting from the analysis of linear systems, which are referred to as the first type of systems in this article, their models are relatively simple, and the state parameters can also be obtained through analytical methods to achieve system state updates. Kalman filtering method is often used for implementation; The second type of system is a conditional nonlinear system, which satisfies Markov processes and has been applied in many military fields. The linear part of the system model can be obtained by analytical methods to obtain system parameters, while the nonlinear part can be estimated by other algorithms. The processing method used is mentioned in reference[7] as a Rao Blackwelled (RBPF) filter based on a combination of particle filtering and Kalman filtering algorithms, The basic idea is to first obtain the parameters of the linear system model state variables under nonlinear partial conditions through the posterior probability distribution in particle filtering, and then use Kalman filters to estimate the parameters of the linear state variables. However, such systems require the use of both linear and nonlinear algorithms, which obviously require a large amount of computation, and the stability and real-time performance of the system often do not meet the requirements.

Therefore, the key to solving the drawbacks of RBPF algorithm, such as high computational complexity, lies in finding a new method to solve the problem of state estimation of nonlinear systems in conditional nonlinear systems. This has also attracted the attention and research of scholars at home and abroad. In reference[8], an extended Kalman filtering algorithm is proposed, which linearizes the nonlinear system model, ignores the integration of high-order terms, but brings calculation errors, Known as truncation error, although it solves the problem of solving the state parameter of nonlinear systems, this algorithm also has lower filtering accuracy due to such errors.

A new combination algorithm based on the combination of unscented Kalman filter and traditional Kalman filter is proposed in reference[9]. The estimation error obtained by Unscented Kalman filter for solving the nonlinear part is much smaller than the probability density approximation method of particle filter algorithm. The idea is to use UT scale transformation, select 2n+1 Sigma points with certain weights, approximate the state parameters in the nonlinear system, usually their mean and covariance, The estimation accuracy of the algorithm is higher than that of traditional particle filtering algorithms and EKF algorithms.

For the singularity of 3D pose parameters and the redundancy of solving high-dimensional pose parameters for non-linear system modeling, the pose estimation of modeling using traditional quaternion parameters as state quantities cannot solve the above problems well. Vathsal[10-11] and others first proposed the quaternion second-order extended Kalman filter (Q-Extended Kalman filter (QEKF)). This algorithm has a low accuracy due to the complexity of the matrix solution. So literatures[12-14] proposed a quaternion-based unscented Kalman filtering algorithm filtering algorithm (Q- unscented Kalman filter, QUKF). However, due to the large selection of Sigma points of the traditional UKF algorithm and the high dimensionality of state quantities,

and those negative weighted Sigma points will cause non-positive definite problems of the algorithm's covariance, the accuracy of the algorithm needs further improvement. In 2009, the idea of generating a brand new set of 2N cubic points with the same weight after a non-linear cubature transformation with a sampling point was proposed, which is the famous cubic Kalman filter (CKF) Algorithm[15]. The algorithm first calculates and propagates the cubature points, through iterative updates of the equation of state, calculating the mean and estimating covariance of observations, and finally calculates the Kalman gain using the cubature radial criterion. Algorithm accuracy is improved compared to previous algorithms.

Although the filtering accuracy of the traditional CKF algorithm has been improved to some extent, when the standard CKF algorithm solves the nonlinear problem of SLAM, with the continuous addition of observation features, the calculation amount increases sharply, and the problem of numerical instability occurs. In this regard, a series of adaptive high-order cubature Kalman filter (HCKF), CDKF and other algorithms have been proposed, but they are basically combined with the covariance matrix to introduce a fading factor to improve the strong tracking ability, but all have their own problem in numerical calculations and filtering accuracy. Combining the ideas of the square root cubature Kalman filter algorithm (SRCKF) proposed in[16-18] etc, a quaternion based square root cubature Kalman filter algorithm (QSRCKF) is proposed.The square root cubature Kalman filter not only reduces the state quantity dimension and computational complexity, but also updates of the square root covariance subtype iteratively which can ensure the non-negative qualitative and symmetry of the algorithm. The new algorithm used in SINS / SLAM integrated navigation can reduce the position error of the carrier and improve the accuracy of carrier attitude estimation.

2. Rationrelated works

In recent years, the author has proposed a square root UKF attitude estimation algorithm based on fuzzy logic quaternion to address the issues of low filtering accuracy during navigation calculation and the inability of traditional quaternion extended Kalman filtering algorithms to meet the accuracy requirements of target attitude measurement in target tracking estimation algorithms, which use sensor discrete observations to estimate the continuous state of the target. This algorithm takes quaternions as the state of the fuzzy logic UKF filter, applies the measured angular rate to complete the time update of the filter, tracks and locates the target in real time, and updates the measurement, suppressing the problem of attitude error divergence. Among them, the fuzzy square root UKF algorithm based on quaternion was compared and analyzed with quaternion UKF and square root quaternion algorithms through simulation experiments, and the position estimation of observed feature targets in the x and y directions was achieved.

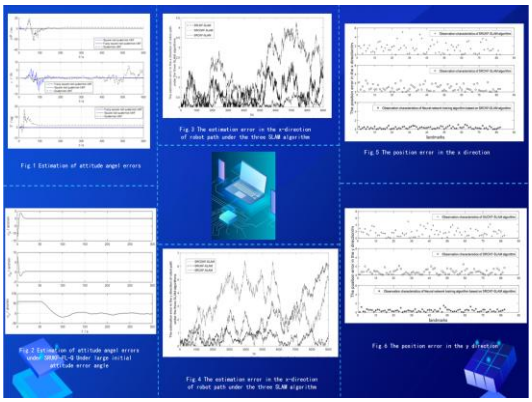

Fig. 1. Carrier attitude estimation error under SRUKF algorithm

From Figure, it can be seen that by changing the initial values of the three types of attitude angles of the carrier, the roll angle and pitch attitude angle errors under this algorithm can approach 0 in a relatively short period of time; Furthermore, as the simulation time progresses, as the yaw angle represents the direction of the carrier's navigation and remains constant for the first 50 seconds, its error also remains unchanged. In the following 50 seconds, its error gradually decreases as well. And achieved the position estimation of observed feature targets in the x and y directions.

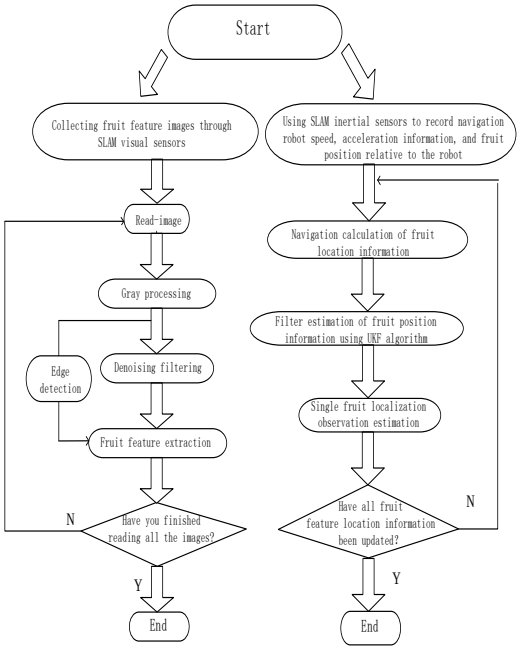

Fig. 2. The overall algorithm flowchart

This paper improves on the SRUKF-SLAM algorithm studied in recent years and proposes a new method for aircraft attitude estimation based on the quaternion SRCKF algorithm. The overall algorithm flowchart[19] is shown in figure 2.

3. Quaternion description of aircraft attitude

Using SINS / SLAM integrated navigation to estimate the attitude of the aircraft can effectively improve the positioning accuracy and strengthen tracking ability. Assumes local coordinate system as global reference $ox_n y_n z_n$ (n)coordinates and carrier coordinate system as $ox_b y_b z_b$ (b)system.Given the reference coordinate system, the rotation order of the carrier system relative to the system is $Z \to X \to Y$. The rotation angles are yaw γ , roll angle α and the pitch attitude angles are β . The attitude rotation matrix of the $n \to b$ system.

$$\begin{aligned} C_n^b &= \begin{bmatrix} \cos\beta & 0 & -\sin\beta \\ 0 & 1 & 0 \\ \sin\beta & 0 & \cos\beta \end{bmatrix} \begin{bmatrix} 1 & 0 & 0 \\ 0 & \cos\alpha & \sin\alpha \\ 0 & -\sin\alpha & \cos\alpha \end{bmatrix} \begin{bmatrix} \cos\gamma & \sin\gamma & 0 \\ -\sin\gamma & \cos\gamma & 0 \\ 0 & 0 & 1 \end{bmatrix} \\ &= \begin{bmatrix} \cos\beta\cos\gamma - \sin\alpha\sin\beta\sin\gamma & \cos\beta\sin\gamma + \sin\alpha\sin\beta\cos\gamma & -\cos\alpha\sin\beta \\ -\cos\alpha\sin\gamma & \cos\beta\cos\gamma & \sin\alpha \\ \sin\beta\cos\gamma + \sin\alpha\cos\beta\sin\gamma & \sin\beta\sin\gamma - \sin\alpha\cos\beta\cos\gamma & \cos\alpha\cos\beta \end{bmatrix} \end{aligned} \tag{1}$$

defines the carrier attitude quaternion as

$$q = \begin{bmatrix} q_1 & q_2 & q_3 & q_4 \end{bmatrix}^T \tag{2}$$

According to the definition of quaternion, satisfy the relationship

$$q^T q = \|q\|^2 = q_1^2 + q_2^2 + q_3^2 + q_4^2 = 1 \tag{3}$$

$$r^b = C_n^b r^n \tag{4}$$

Then through the coordinate rotation relationship and quaternion rotation theory, it can be calculated the quaternion's attitude transformation matrix for the carrier in $n \to b$ system is

$$C_n^b = \begin{bmatrix} q_1^2 + q_2^2 - q_3^2 - q_4^2 & 2(q_2 q_3 + q_1 q_4) & 2(q_2 q_4 - q_1 q_3) \\ 2(q_2 q_3 - q_1 q_4) & q_1^2 + q_3^2 - q_2^2 - q_4^2 & 2(q_1 q_2 + q_3 q_4) \\ 2(q_1 q_3 + q_4 q_2) & 2(q_3 q_4 - q_1 q_2) & q_1^2 + q_4^2 - q_2^2 - q_3^2 \end{bmatrix} \tag{5}$$

According to the transformation relationship between the Euler angle attitude matrix and the quaternion attitude matrix, the carrier attitude angle is calculated as

$$\begin{cases} \alpha = \arctan 2\left[2\left(q_1 q_2 + q_3 q_4\right) \quad \sqrt{4\left(q_2 q_4 - q_1 q_3\right)^2 + \left(q_1^2 + q_4^2 - q_2^2 - q_3^2\right)^2} \right] \\ \beta = \arctan\left[2\left(q_2 q_4 - q_1 q_3\right) \quad \sqrt{4\left(q_1 q_2 + q_3 q_4\right)^2 + \left(q_1^2 + q_4^2 - q_2^2 - q_3^2\right)^2} \right] \\ \gamma = \arctan 2\left[2\left(q_2 q_3 - q_1 q_4\right) \quad q_1^2 + q_2^2 - q_3^2 - q_4^2 \right] \end{cases} \tag{6}$$

3.1. Gyro Quaternion Model

Suppose the real angular velocity of the carrier relative to the reference frame is According to the rigid body rotation theorem, the quaternion differential equation of the attitude of the carrier can be obtained as:

$$\dot{q} = \frac{1}{2}\Omega_{nb}^{b} q \tag{7}$$

among them $\Omega_{nb}^{b} = \begin{bmatrix} 0 & -\omega_{nbx}^{b} & -\omega_{nby}^{b} & -\omega_{nbz}^{b} \\ \omega_{nbx}^{b} & 0 & \omega_{nbz}^{b} & -\omega_{nby}^{b} \\ \omega_{nby}^{b} & -\omega_{nbz}^{b} & 0 & \omega_{nbx}^{b} \\ \omega_{nbz}^{b} & \omega_{nby}^{b} & -\omega_{nbx}^{b} & 0 \end{bmatrix}$.

Under ideal conditions, the quaternion state equation is:

$$q_k = q_{k-1} + \frac{\Delta t}{2}\Omega_{k|k-1} q_{k-1} \tag{8}$$

Among them, Δt is the angular velocity sampling period.

The measured gyroscope output is ω_{ib}^{b} including real angular velocity ω_{nb}^{b} and gyroscope random drift ω_{in}^{b} . That is $\omega_{ib}^{b} = \omega_{nb}^{b} + \omega_{in}^{b}$ so the gyroscope model is expressed as:

$$\omega_{nb}^{b} = \omega_{ib}^{b} - \omega_{in}^{b} = \omega_{ib}^{b} - C_{n}^{b}\omega_{in}^{n} \tag{9}$$

Where, ω_{in}^{n} is the value of the gyro drift in the reference n frame.

The quaternion output of the CCD star sensor is used as the gyroscope attitude measurement. It is assumed that the direction of the angular velocity is fixed during adjacent times. The discrete equation of the kinematics of the carrier represented by the quaternion is:

$$q_{k+1} = \Omega\left(\omega_k\right) q_k = \begin{bmatrix} \cos\left(\frac{1}{2}\|\omega_k\|\Delta t\right) I_{3\times 3} - \left[\psi_k^{\times}\right] & \psi_k \\ -\psi_k^{T} & \cos\left(\frac{1}{2}\|\omega_k\|\Delta t\right) I_{3\times 3} \end{bmatrix} \tag{10}$$

In this formula $\psi_k = \sin\left(\frac{1}{2}\|\omega_k\|\Delta t\right)\omega_k \Big/ \|\omega_k\|$, $\left[\psi_k^{\times}\right]$ is the antisymmetric matrix for ψ_k.

Expand the quaternion differential equation in equation (7):

$$\dot{q} = \frac{1}{2}\Omega(\omega)q = \frac{1}{2}\begin{bmatrix} 0 & -\omega_x & -\omega_y & -\omega_z \\ \omega_x & 0 & \omega_z & -\omega_y \\ \omega_y & -\omega_z & 0 & \omega_x \\ \omega_z & \omega_y & -\omega_x & 0 \end{bmatrix} q \tag{11}$$

The gyroscope is used to measure the angular velocity of the carrier. The state model is:

$$\begin{cases} \omega_g = \begin{bmatrix} \omega_x & \omega_y & \omega_z \end{bmatrix}^T = \hat{\omega} - b - \xi_a \\ \dot{b} = \xi_b \end{cases} \tag{12}$$

In this formula ω_g is the true angular velocity. $\hat{\omega}$ is the actual gyroscope output value. b is the gyroscope drift error and ξ_a、ξ_b is the system's white Gaussian noise which meets $\xi_a \sim N\left(0, \sigma_a^2\right)$, $\xi_b \sim N\left(0, \sigma_b^2\right)$.

3.2. Star sensor observation model

The star sensor measurement model is described as:

$$z_k = H\left(q_k\right)r + v_k \tag{13}$$

In this formula z_k is the output of the star sensor; $H\left(q_k\right)$ is the attitude matrix of the star sensor at all times; is the reference vector of the star sensor; and is the zero mean Gaussian white noise.

4. SRCKF-SLAM algorithm based on quaternion

Let the system state quantity and covariance matrix in the SLAM model be:

$$x = \begin{bmatrix} x_v & x_m \end{bmatrix},\ P = \begin{bmatrix} P_{vv} & P_{vm} \\ P_{vm}^T & P_{mm} \end{bmatrix}.$$

Where, x_v, x_m are carrier state and map feature state respectively, and each contains two-dimensional position information in the direction x, y. P_{vv}, P_{vm}, P_{mm} are the carrier autocorrelation covariance matrix, the carrier and map feature cross-covariance matrix, and the map feature autocovariance matrix respectively.

Under control input u_k, consider the SLAM problem as the state quantity and the posterior joint probability density problem:

$$p\left(x_{v,k}, x_m \mid z_k, u_k\right) = p\left(z_k \mid x_{v,k}, x_m\right) \cdot \int p\left(x_{v,k} \mid x_{v,k-1}, u_k\right) \cdot p\left(x_{v,k-1}, x_m \mid z_{k-1}, u_{k-1}\right) dx_{v,k-1} \tag{14}$$

In this formula, $p\left(x_{v,k} \mid x_{v,k-1}, u_k\right)$ is a motion model and $p\left(z_k \mid x_{v,k}, x_m\right)$ is a measurement model. The general nonlinear motion model can be expressed as:

$$\begin{cases} x_k = f\left(x_{k-1}\right) + w_k \\ z_k = h\left(x_k\right) + v_k \end{cases} \tag{15}$$

In this formula, $f(\cdot)$ and $h(\cdot)$ are nonlinear system function and observation function. Uncorrelated system Gaussian white noise and observed Gaussian white noise are $w_k \sim N(0, Q)$、$v_k \sim N(0, R)$.

4.1. SRCKF algorithm update steps

State parameter initialization

$$\begin{cases} \hat{x}_0 = E\left[x_0\right], P_0 = E\left[\left(x_0 - \hat{x}_0\right)\left(x_0 - \hat{x}_0\right)^T\right] \\ S_0 = \mathrm{Chol}\left\{E\left[\left(x_0 - \hat{x}_0\right)\left(x_0 - \hat{x}_0\right)^T\right]\right\} \end{cases} \tag{16}$$

In this formula, Chol represents matrix Cholesky's factorization.

(1)Time update

Set $k-1$time joint posterior probability $P\left(x_{k-1}\right) = N\left(\hat{x}_{k-1|k-1}, P_{k-1|k-1}\right)$ known, through Cholesky decomposes error covariance $P_{k-1|k-1} = S_{k-1|k-1} S_{k-1|k-1}^T$ · $S_{k-1|k-1}$ is the error covariance equation in the formula.

①Use dimension n point cubature to generate dimension $2n$ clllection of cubature points:

$$x_{i,k-1} = S_{k-1}\varepsilon_i + \hat{x}_{k-1} \tag{17}$$

In the formula, $\varepsilon_i = \sqrt{n}\left[1\ \right]_{2n}$ is the point of origin. The corresponding weights for each cubature point are: $\tau_i = \frac{1}{2n}$, $i = 1, 2, \mathrm{L}\ , 2n$.

②Propagate the cubature point and calculate the state prediction value:

$$x_{i,k|k-1}^* = f\left(x_{i,k-1}\right) \tag{18}$$

$$\hat{x}_{k|k-1} = \sum_{i=1}^{2n} \tau_i x_{i,k-1}^* \tag{19}$$

③Calculate the predicted value of state error covariance:

$$P_{k|k-1}=\tau_i\sum_{i=1}^{2m}\left(x^*_{k|k-1}x^{*T}_{k|k-1}-\hat{x}_{k|k-1}\hat{x}^{*T}_{k|k-1}+Q_{k-1}\right) \tag{20}$$

Rewrite Q_{k-1} to Cholesky decomposition:

$$Q_{k-1}=S_{Q,k-1}S^T_{Q,k-1} \tag{21}$$

④State error covariance equation:

$$\begin{cases} S_{k|k-1}=qr\left[\chi_{k|k-1}\quad S_{Q_{k-1}}\right] \\ \chi^*_{k|k-1}=\dfrac{1}{\sqrt{2n}}\left[x^{*,1}_{k|k-1}-\hat{x}_{k|k-1},x^{*,2}_{k|k-1}-\hat{x}_{k|k-1},\right. \\ \left.\mathrm{L}\ ,x^{*,2n}_{k|k-1}-\hat{x}_{k|k-1}\right] \end{cases} \tag{22}$$

In the formula, qr is the decomposition of QR matrix.

(2)Measurement update

①Calculate the cubature point

$$x_{i,k|k-1}=S_{k|k-1}\varepsilon_i+\hat{x}_{k|k-1},\ i=1,2,\mathrm{L}\ ,2n \tag{23}$$

②Propagation cubature point

$$z^*_{i,k|k-1}=h\left(x_{i,k|k-1}\right) \tag{24}$$

③Calculate the predicted value of observation at k time:

$$\hat{z}_{k|k-1}=\frac{1}{2n}\sum_{i=1}^{2n}z^*_{k|k-1} \tag{25}$$

④Calculate autocorrelation covariance

$$P_{zz,k|k-1}=\tau_i\sum_{i=1}^{2n}\left(z_{i,k|k-1}z^T_{i,k|k-1}-\hat{z}_{i,k|k-1}\hat{z}^T_{i,k|k-1}+R_k\right) \tag{26}$$

Rewrite R_{k-1} into Cholesky decomposition

$$R_{k-1}=S_{R,k-1}S^T_{R,k-1} \tag{27}$$

Covariance square root error:

$$\begin{cases} S_{zz,k|k-1}=qr\left[\eta_{k|k-1}\quad S_{R_k}\right] \\ \eta_{k|k-1}=\dfrac{1}{\sqrt{2n}}\sum_{i=1}^{2n}\left(\begin{matrix} z^{*,1}_{i,k|k-1}-\hat{z}_{k|k-1},z^{*,2}_{i,k|k-1}-\hat{z}_{k|k-1}, \\ \mathrm{L}\ ,z^{*,2n}_{i,k|k-1}-\hat{z}_{k|k-1}\end{matrix}\right) \end{cases} \tag{28}$$

The square root of the estimated (weight) cross-covariance is

$$\begin{cases} \chi_{k|k-1}=\dfrac{1}{\sqrt{2n}}\left[\begin{matrix} x^1_{k|k-1}-\hat{x}_{k|k-1},x^2_{k|k-1}-\hat{x}_{k|k-1}, \\ \mathrm{L}\ ,x^{2n}_{k|k-1}-\hat{x}_{k|k-1}\end{matrix}\right] \\ P_{xz,k|k-1}=\chi_{k|k-1}\eta^T_{k|k-1} \end{cases} \tag{29}$$

Kalman gain is:

$$K_k = \left(P_{xz,k|k-1} / S_{zz,k|k-1}^T \right) S_{zz,k|k-1} \tag{30}$$

Correlation state root square error

$$S_{k|k} = qr\left[\chi_{k|k-1} - K_k \eta_{k|k-1}, \;\; k_k S_{R,k} \right] \tag{31}$$

Four-element SRCKF select attitude error $\delta x_{i,k-1}^q$ and gyro drift error $\delta x_{i,k-1}^{\mathrm{b}}$ to make joint status:

$$\delta x_{i,k-1} = \left[\delta x_{i,k-1}^q, \delta x_{i,k-1}^{\mathrm{b}} \right]^T = S_{k-1} \varepsilon_i, \quad i = 1,2,\mathrm{L}\ ,2n \tag{32}$$

The quaternion SRCKF state cubature points are

$$\begin{cases} x_{i,k-1}^q = \delta \hat{q}_{i,k-1} \otimes \hat{q}_{k-1} \\ x_{i,k-1}^{\mathrm{b}} = \hat{x}_{k-1}^{\mathrm{b}} + \delta \hat{x}_{i,k-1}^{\mathrm{b}} \end{cases} \tag{33}$$

Define the error quaternion as

$$\delta x_{i,k-1}^q = \hat{q}_{k|k-1} \otimes \left(x_{i,k-1}^q \right)^{-1} \tag{34}$$

4.2. SRCKF-SLAM algorithm update steps

(1) Update the quaternion SRCKF-SLAM time:

$$\begin{cases} x_{i,k|k-1} = f\left(x_{i,k-1} \right) \\ \hat{\mathrm{b}} = \sum_{i=1}^{2n} \tau_i x_{i,k|k-1}^{\mathrm{b}} \\ S_{k|k-1}^q = qr\left[\chi_{q,k|k-1}^* \quad S_{Q_{k-1}}^q \right] \\ S_{k|k-1}^{\mathrm{b}} = qr\left[\chi_{\mathrm{b},k|k-1}^* \quad S_{Q_{k-1}}^{\mathrm{b}} \right] \\ S_{k|k-1}^{q,\mathrm{b}} = qr \begin{bmatrix} \tau_i \delta x_{k|k-1}^{q,1} \left(x_{k|k-1}^{\mathrm{b},1} - \hat{\mathrm{b}}_{k|k-1} \right)^T \\ \tau_i \delta x_{k|k-1}^{q,2} \left(x_{k|k-1}^{\mathrm{b},2} - \hat{\mathrm{b}}_{k|k-1} \right)^T \\ \mathrm{M} \\ \tau_i \delta x_{k|k-1}^{q,2n} \left(x_{k|k-1}^{\mathrm{b},2n} - \hat{\mathrm{b}}_{k|k-1} \right)^T \end{bmatrix}^T \\ S_{k|k-1} = \begin{bmatrix} S_{k|k-1}^q & S_{k|k-1}^{q,\mathrm{b}} \\ \left(S_{k|k-1}^{q,\mathrm{b}} \right)^T & S_{k|k-1}^{\mathrm{b}} \end{bmatrix} \end{cases} \tag{35}$$

Where, $\hat{\mathrm{b}}$ is the predicted value for gyro drift part, $S_{k|k-1}^q$、$S_{k|k-1}^{\mathrm{b}}$ are square root covariance sub-forms for pose estimation and gyro drift error, and

$$\begin{cases} \chi^{*}_{q,k|k-1}=\dfrac{1}{2n}\left[\delta x^{q,1}_{k|k-1},\delta x^{q,2}_{k|k-1},\mathrm{L}\ ,\delta x^{q,2n}_{k|k-1}\right] \\ \chi^{*}_{\mathrm{b},k|k-1}=\dfrac{1}{2n}\begin{bmatrix} x^{\mathrm{b},1}_{k|k-1}-\hat{b}_{k|k-1},x^{\mathrm{b},2}_{k|k-1}-\hat{b}_{k|k-1}, \\ \mathrm{L}\ ,x^{\mathrm{b},2\mathrm{n}}_{k|k-1}-\hat{b}_{k|k-1} \end{bmatrix} \end{cases} \tag{36}$$

Update the quaternion SRCKF-SLAM measurement:

①Update the quaternion SRCKF state cubature point:

$$\xi^{q}_{i,k|k-1}=\delta z^{q}_{i,k|k-1}\otimes\hat{q}_{k|k-1} \tag{37}$$

②Measurement update and error auto-covariance sub-form and cross-covariance update

$$\begin{cases} z^{q}_{i,k-1}=\delta\hat{q}_{i,k-1}\otimes\xi^{q}_{i,k|k-1}\otimes\hat{q}_{k-1} \\ \delta z_{i,k}=S_{k|k-1}\varepsilon_{i}=\left[\delta z^{q}_{i,k-1},\delta z^{\mathrm{b}}_{i,k-1}\right]^{T} \\ S_{zz,k}=qr\left[\eta_{z,k}\quad S^{\eta}_{R_{k-1}}\right] \\ P_{xz,k}=\begin{bmatrix} \tau_{i}\sum\limits_{i=1}^{2n}\delta x^{q}_{k|k-1}\left(\delta z^{q}_{k|k-1}\right)^{T} \\ \tau_{i}\sum\limits_{i=1}^{2n}\left(x^{\mathrm{b}}_{i,k|k-1}-\hat{\mathrm{b}}_{k|k-1}\right)\left(\delta z^{q}_{i,k|k-1}\right)^{T} \end{bmatrix}^{T} \end{cases} \tag{38}$$

$$\begin{cases} \delta z^{q}_{i,k-1}=\hat{z}_{k|k-1}\otimes\left(\delta z^{q}_{i,k-1}\right)^{-1} \\ \eta_{z,k}=\dfrac{1}{2n}\left[\delta z^{q,1}_{k},\delta z^{q,2}_{k},\mathrm{L}\ ,\delta z^{q,2n}_{k}\right] \end{cases} \tag{39}$$

Kalman gain:

$$K_{k}=\left(P_{xz}/S^{T}_{zz,k}\right)\cdot\frac{1}{S_{zz,k}} \tag{40}$$

State error amount:

$$\delta\hat{x}_{k}=K_{k}\delta\hat{z}_{k|k-1} \tag{41}$$

Where, $\begin{cases} \delta\hat{x}_{k}=\left[\delta\hat{q}^{T}_{k}\quad\delta\hat{b}^{T}_{k}\right]^{T} \\ \delta\hat{z}_{k|k-1}=z_{k}\otimes\left(\hat{z}_{k|k-1}\right)^{-1}\cdot \\ \delta\hat{q}_{k}=\dfrac{\delta\hat{q}_{k}}{\left\|\delta\hat{q}_{k}\right\|_{2}} \end{cases}$

③Gyro drift update

$$\begin{cases} \hat{q}_{k}=\delta\hat{q}_{k}\otimes\hat{q}_{k|k-1} \\ \hat{b}_{k}=\hat{b}_{k|k-1}+\delta\hat{b}_{k} \end{cases} \tag{42}$$

The state quantity error covariance matrix is:

$$S_k = chol\left(S_k S_{k|k-1}^T, U_k U_k^T, -1\right) \tag{43}$$

Where, $U_k = K_k S_{zz,k}$.

5. Simulation experiments and analysis

5.1. Comparison of Three Filtering Algorithms for Attitude Angle Estimation

Taking a near-Earth satellite as an example, a star sensor is installed vertically, and a SINS / SLAM integrated navigation and CCD attitude estimation system platform is established, and tested in Matlab and C ++ software. Assumed satellite orbit altitude is 800Km and the inclination angle is 82 °. The initial position of the aircraft is 114 ° E, 36 ° N. Initial attitude angle error and initial gyro drift are zero. The gyro initial drift error variance matrix is $\mathrm{diag}\left(0.2, 0.2, 0.2\right)_{3\times3}$. The initial attitude angle error variance matrix is $\mathrm{diag}\left(0.25, 0.25, 0.25\right)_{3\times3}$. The initial process noise is $\mathrm{diag}(0.02^2 I_{3\times3}, 0.05^2 I_{3\times3})$. The initial measurement noise variance matrix is $\mathrm{diag}\left[20, 20, 20\right]_{3\times3}$. The simulation time is 600s, and other parameters are shown in Table 1.

Table 1. Parameters of aircraft and gyros

Parameter	Value	Parameter	Value
Satellite orbital angular velocity	0.001rad/s	Gyro constant drift error	$0.1°/h$
Satellite initial attitude angular velocity	$[0.1\ 0.1\ 0.1]^{\mathrm{T}}$(°/s)	Gyro drift standard deviation of noise	$0.02\left(°/\sqrt{\mathrm{h}}\right)$
Satellite three-axis initial attitude angle	$[0\ 0\ 5]^{\mathrm{T}}$(°)	Gyroscope measurement standard deviation of noise	$0.05\left(°/\sqrt{\mathrm{h}}\right)$
Satellite triaxial initial error angle	$[0.5\ 0.5\ 5]^{\mathrm{T}}$(°)	Gyroscope output frequency	50Hz
Star sensor Output frequency	2Hz	Star sensor measuring noise	$N\left(0, 20''\right)$
Satellite orbital angular velocity	0.001rad/s	Gyro constant drift error	$0.1°/h$

In order to verify the superiority of the proposed algorithm based on SLAM nonlinear model estimation accuracy, this experiment compared the quaternion SRUCF-SLAM and quaternion SRCDKF-SLAM algorithms to estimate the roll attitude angle error, pitch attitude angle error, and flight The magnitude of the deviation attitude error, and the simulation results are shown in figures 3 to 5:

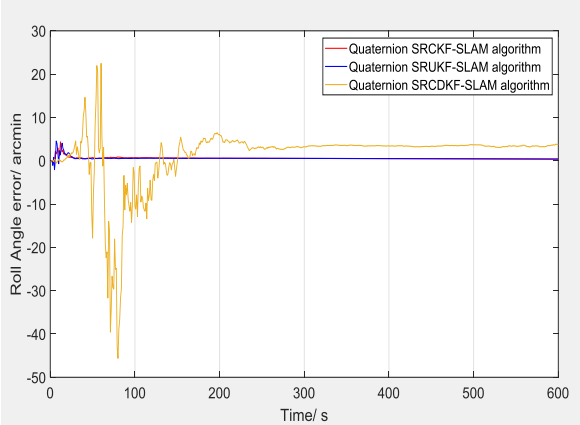

Fig. 3. Roll angle error

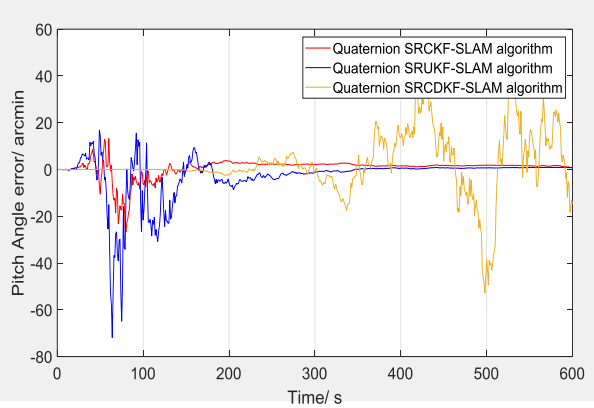

Fig. 4. Pitch angle error

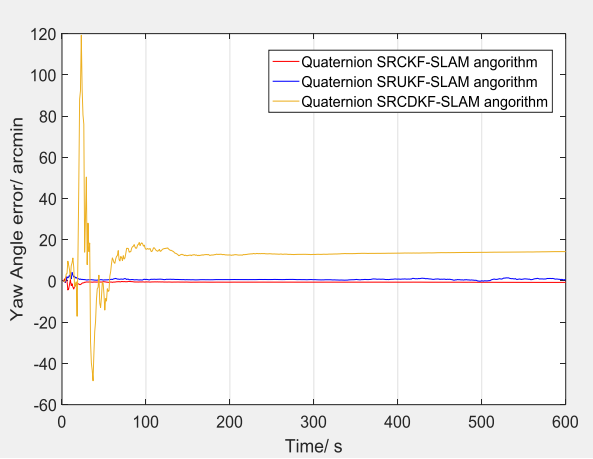

Fig. 5. Yaw angle error

As can be seen from Figures 3, 4, and 5, given the initial conditions, the estimation error based on the quaternion SRCDKF-SLAM is the largest for the roll attitude and yaw attitude angle estimates, and the quaternion SRCKF- SLAM algorithm has almost the same filtering accuracy as the quaternion SRUKF-SLAM algorithm.

However, the computational complexity of the former is smaller than that of the latter, and the numerical stability is higher.

For pitch attitude estimation, it is clear that the quaternion SRCKF-SLAM has the smallest error, and can quickly converge to zero, with the best stability.

The mean statistics of the attitude angle estimation errors of the three filtering algorithms are shown in Table 2:

Table 2. Comparison of performance based of three algorithms

Algorithm parameter	Quaternion SRCDKF-SLAM	Quaternion SRUKF-SLAM	Quaternion SRCKF-SLAM
Rolling angle error mean	8″	4″	3″
Absolute mean value of pitch error	19″	6″	5″
Absolute mean value of heading error	24″	4″	2″
Time spent in one iteration	0.028s	0.036s	0.012s

As can be seen from Table 3, the estimation errors of the quaternion SRCDKF-SLAM algorithm, quaternion SRUCF-SLAM algorithm, and quaternion SRCCKF-SLAM algorithm decrease sequentially, and the new algorithm has the shortest iteration time and the strongest time-consuming performance, which is consistent with simulation graphics.

5.2. Experimental simulation and analysis under conditions of large initial error angle

The quaternion SRCDKF and quaternion SRUKF algorithms have large errors in attitude angle estimation, which leads to a large proportion of the vertical coordinate of the three filtering simulation graphics. Robustness and filtering accuracy. In this set of experiments, the initial roll angle attitude angle error, pitch attitude angle error, and yaw attitude angle error are 30 arcmin, 30 arcmin, and 60 arcmin, respectively. The initial conditions of the gyroscope are consistent with 5.1, the simulation time is 300s, and the simulation graph is shown in Figure 6:

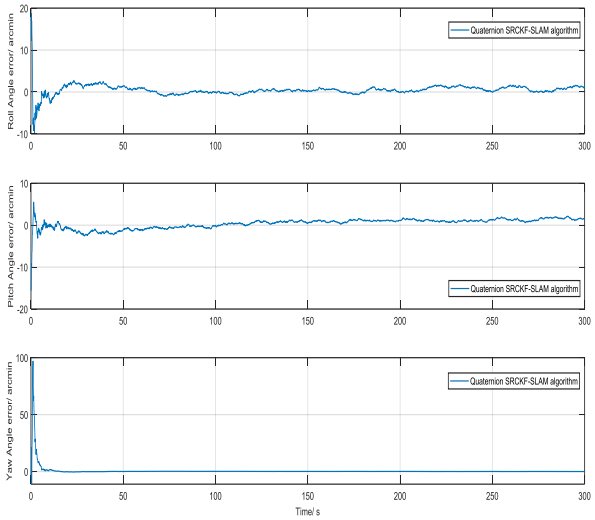

Fig. 6. Quaternion SRCKF-SLAM attitude angle estimation error

It can be seen from Figure 4 that given a large initial error attitude angle, the estimation error of the attitude angle based on the quaternion SRCKF-SLAM algorithm can be quickly reduced to about 50 in the first 50s of the simulation time, and the convergence speed is fast. And as the simulation time progresses, the filtering always remains stable, which shows that the algorithm has strong robustness and stability for large misalignment attitude angle filtering estimation.

5.3. Computer simulation experiment verification and analysis

In order to verify the effectiveness and feasibility of the SLAM algorithm proposed in this article, MATLAB simulation was conducted. The simulation environment was set up in the open-source SLAM simulator released by scholar Tim Bailey from the University of Sydney. The experimental environment is located in an outdoor environment area of 100 m ×100 m, including the actual operation path of the carrier set artificially and 10 stationary road signs. The carrier moves clockwise along the simulated and actually determined trajectory from the coordinates of (60, 10). The specific experimental environment is shown in Figure 7.

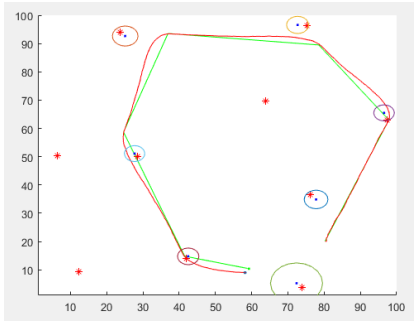

Fig. 7. Experimental environment

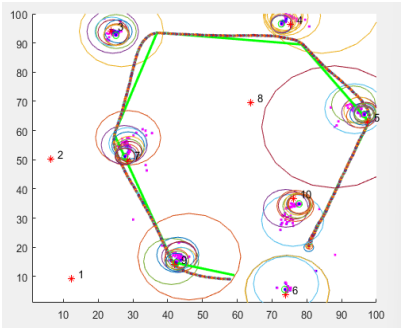

Fig. 8. SLAM feature observation

In Figure 7, the green line represents the actual navigation path of the robot, the red line represents the estimated tracking path of the robot under the SLAM algorithm, and the * point represents the 10 actual feature target objects present in the simulation area. In Figure 8, the actual observations of 10 feature targets by the SLAM algorithm in robot position tracking estimation are shown. The experimental results show that when the robot moves along the specified path, based on data fusion and observation in the SLAM algorithm, the 3rd, 4th, 5th, 6th, 7th, 9th, and 10th feature points under the navigation path are finally observed. Multiple judgments are made for each observation, and the position of the effective observation point is ultimately determined.

5.4. Analysis of cumulative error in inertial navigation systems

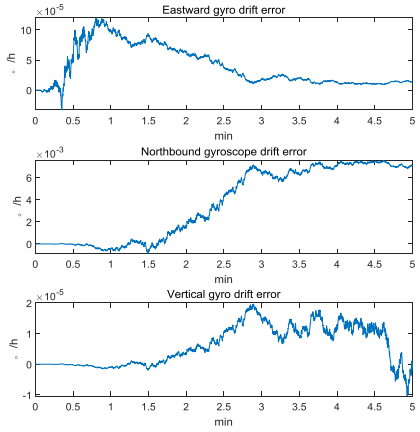

Fig. 9. Gyroscope drift error

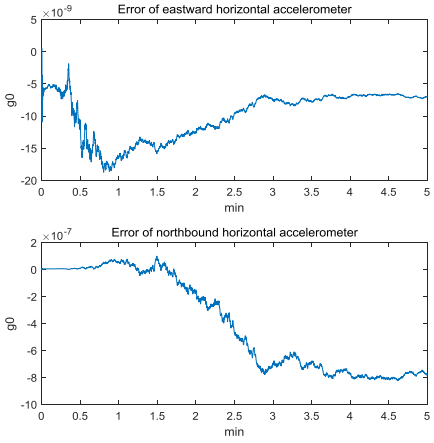

Fig. 10. Accelerometer drift error

In figure 9, the cumulative errors of the system gyroscope in three directions under inertial navigation are shown, and their mean errors are relatively large. If not combined with other navigation algorithms, this error will accumulate over time, leading to a gradual increase in carrier positioning error.

Figure 10 showed the parameter estimation of another inertial device accelerometer, and it can be seen that its error gradually accumulates over time. One integration leads to the accumulation of velocity error, while the second integration leads to the accumulation of position error. Therefore, a combination of other positioning methods must be used to weaken the above two drift errors.

5.5. Estimation of UAV position error under three filtering algorithms

Under the above experimental environment, 50 independent repeated simulation experiments were conducted on SRCKF-SLAM, SRUKF-SLAM, and SRCDKF-SLAM, and the estimation errors in the direction of the carrier path were analyzed and compared. The results are shown in the figure 11-13.

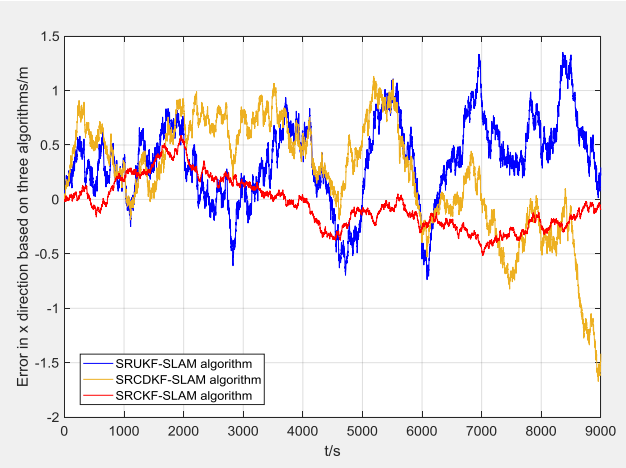

Fig. 11. Error in x direction based on three algorithms

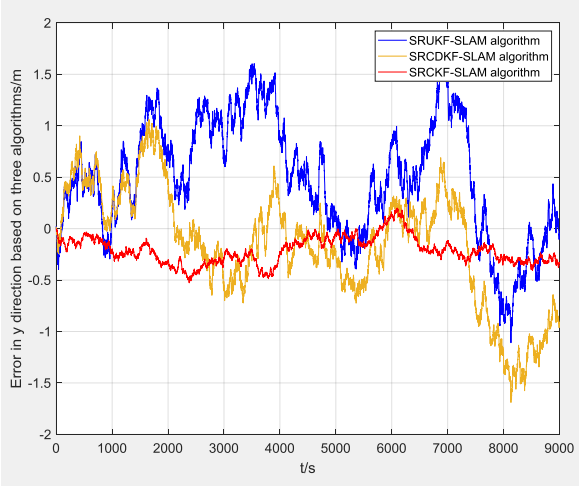

Fig. 12. Error in y direction based on three algorithms

From figure 11, it can be seen that the error range of the SRCKF-SLAM algorithm in the x-direction of the navigation trajectory of the plant protection unmanned aerial vehicle is approximately [-0.5,0.6] m. The errors of the SRUKF-SLAM algorithm and the SRCDKF-SLAM algorithm are approximately [-0.7,1.4] m and [-1.7,1.2] m. It can

be seen that the former has the smallest mean estimation error in the x-direction of the unmanned aerial vehicle, the smallest error fluctuation range, and the best stability.

From figure 12, it can be seen that the error range of the SRCKF-SLAM algorithm in the y-direction of the navigation trajectory of the plant protection UAV is approximately [-0.5,0.2] m. The errors of the SRUKF-SLAM algorithm and the SRCDKF-SLAM algorithm are approximately [-1.15,1.6] m and [-1.7,1.1] m, respectively. It can be seen that the former has the smallest mean position estimation error in the y-direction of the drone, the smallest error fluctuation range, and the best stability. The error based on the SRCDKF-SLAM algorithm is the largest, and the filtering fluctuation amplitude is also the largest, followed by the error of the SRUKF-SLAM algorithm.

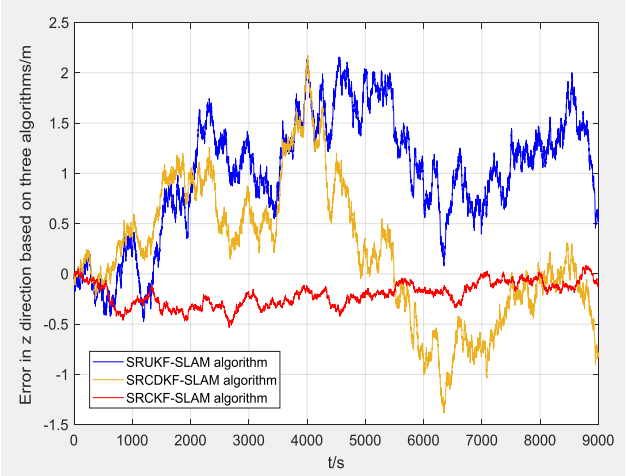

Fig. 13. Error in z direction based on three algorithms

From figure 13, it can be seen that the error range of the SRCKF-SLAM algorithm for the z-direction navigation trajectory of the plant protection UAV is approximately [-0.5,0.05] m. The errors of the SRUKF-SLAM algorithm and the SRCDKF-SLAM algorithm are approximately [-0.5,2.2] m and [-1.45,2.2] m, respectively. From this, it can be seen that the former has the smallest average position estimation error in the z-direction of the UAV, and its error positions are within a small range throughout the entire simulation time, It shows that the UAV for plant protection can perform spraying operation at a constant height at a basic position, and has high stability. The filtering algorithm has strong Uniform convergence. The error based on the SRCDKF-SLAM algorithm is the largest, and the filtering fluctuation amplitude is also the largest, followed by the error of the SRUKF-SLAM algorithm.

6. Discussion

This article mainly discusses the carrier attitude estimation based on three filtering algorithms, including quaternion based SRCKF, and provides several comparative experiments to verify that quaternion based SRCKF-SLAM algorithm has the highest

estimation accuracy, and its computational complexity is slightly reduced compared to the other two algorithms. However, more comparisons between algorithms still need to be validated. These will be subject to further research.

7. Conclusions

This article proposes a quaternion based SRCKF algorithm to address the problems of complex navigation solutions, high computational complexity, unstable filtering, and poor accuracy in traditional quaternion SRUKF and SRCDKF algorithms. The algorithm is applied to a nonlinear model of SLAM, and simulation experiments are conducted on three initial attitude angle errors under the same conditions. The results show that the new algorithm has a mean estimation error for carrier roll angle, pitch angle, and yaw angle, which are 0.05 °, 0.08 °, 0.03 °,respectively. Compared with the quaternion SRUKF-SLAM algorithm, the accuracy of the algorithm is improved by about 30%. In addition, given the large misalignment angle error, the estimation performance of the quaternion SRCKF-SLAM is examined. Experiments show that the filtering error of the algorithm can be quickly reduced to about 50 in the first 50s of the simulation time, and the convergence speed is fast. As the simulation time progresses, the filtering always remains stable, showing strong robustness and convergence.

The position error estimation experiment on the navigation trajectory of a plant protection UAV shows that the SRCKF-SLAM algorithm has the smallest mean filtering error in three directions, the smallest error fluctuation range, and the best convergence.

Although multiple filtering algorithms were compared and achieved high carrier localization accuracy in the experiments conducted throughout the article, further improvements are still needed for the algorithms mentioned in the paper. For example, combining neural networks or deep learning methods to train the volume points in the volume Kalman filter, and updating the time and measurement of parameters such as mean and covariance, in order to achieve faster, more stable, and more robust filtering results.

Acknowledgment. This research was funded by Henan Provincial Science and Technology Research Project, China (182102110295). Key Scientific Research Project of Colleges and Universities in Henan Province, China (21A590001). Key Scientific Research Project of Colleges and Universities in Anhui Province, China (2023AH051547, 2023AH051559). Key projects of Anyang Institute of technology's 2020 scientific research and Cultivation Fund, China (YPY2020001). The project of cultivating excellent young teachers of Anhui province, China (YQYB2023031). Teaching Quality Engineering Project of Anhui province, China (2023jyxm0796). Teaching Quality Engineering Project of Huainan Normal University, China (2023hskc06). Guiding Science and Technology Plan Project of Huainan Science and Technology Bureau (126).

Thank you for the funding from the Anhui Province Joint Construction Discipline Key Laboratory. Especially the support of the aircraft simulation platform, which has provided basic support for the experiment in this paper.

References

1. Zhao Y, Yang S, Jia R, et al. The statistical observation localized equivalent-weights particle filter in a simple nonlinear model. Acta Oceanologica Sinica, Vol. 41, No. 2:80-90, doi:10.1007/s13131-021-1876-1,(2022).
2. Cao H Q, Nguyen H X, Tran T N C, et al. A Robot Calibration Method Using a Neural Network Based on a Butterfly and Flower Pollination Algorithm.IEEE Transactions on Industrial Electronics,Vol. 69, No. 4:3865-3875. doi:10.1109/TIE. 2021.3073312,(2021).
3. Feng K, Li J, Zhang X, et al. A new quaternion-based Kalman filter for real-time attitude estimation using the two-step geometrically-intutive correction algorithm. Sensors, Vol. 17, No. 11:2530-1545, doi:10.3390/s17092146,(2017).
4. Min Y, Xiong Z, Xing L, et al. An improved SINS/GNSS/CNSS federal based on dual quaternions. Acta Armamentari,Vol. 39, No. 2, 315-324, doi:10.3969/j.issn.1000-1093.2018.02.014,(2018).
5. Yin S, Li H, Sun Y, et al. Data Visualization Analysis Based on Explainable Artificial Intelligence: A Survey. IJLAI Transactionss on Science and Engineering, Vol. 2, No. 3: 24–31. http://ijlaitse.com/index.php/site/article/view/34,(2024).
6. Jiang, Y., Yin, S. Heterogenous-view Occluded Expression Data Recognition Based on Cycle-Consistent Adversarial Network and K-SVD Dictionary Learning Under Intelligent Cooperative Robot Environment. Computer Science and Information Systems, Vol. 20, No. 4. https://doi.org/10.2298/CSIS221228034J,(2023).
7. Zhang H, Qin W, Zhou C, et al. Attitude Determination Algorithm for Micro-satellite Based on High-order UKF Using Information Fusion. Vol. 40, No. 6:1091-1101. doi:10.11728/cjss2020.06.1091,(2020).
8. Zhao Y, Liu Q. Causal ML:Python package for causal inference machine learning. SoftwareX, Vol. 21:101294. doi: org/10.1016/j.softx.2022.101294,(2023).
9. Jia R. Attitude estimation algorithm for low cost MEMS based on quaternion EKF. Chinese Journal Of Sensors And Acthators,Vol. 27, No. 1:90-95, doi:10.3969/j.issn.1004-1699.2014.01.017,(2014).
10. Luo X, Zhou M, Li S, et al.Non-Negativity Constrained Missing Data Estimation for High Dimensional and Sparse Matrices from Industrial Applications. IEEE transactions on cybernetics, Vol. 50, No. 5:1844-1855. doi:10.1109/TCYB.2019.2894283,(2020).
11. Wang D, Tan K, Dong Y, et al. Estimating the position and orientation of a mobile robot using neural network framework based on combined square-root cubature Kalman filter and simultaneous localization and mapping. Advances in Production Engineering & Management, Vol.15, No. 1:31-43. doi:10.14743/apem2020.1.347,(2020).
12. Xiong Y, Zhang Y, Guo X, et al. Seamless global positioning system/inertial navigation system navigation method based on square-root cubature Kalman filter and random forest regression. Review of Scientific Instruments, Vol.90, No.1:015101, doi: 10.1063/1.5079889,(2019).
13. Li Y, Fu K, Sun H. An Aircraft Detection Framework Based On Reinforcement Learning and Convolutional Neural Networks in Remote Sensing Images. Remote Sensing, Vol.10, No.1:243-262. doi: 10.3390/rs10020243,(2018).
14. Dai, Y., Xu, B., Yan, S., Xu, J. Study of cardiac arrhythmia classification based on convolutional neural network. Computer Science and Information Systems, Vol. 17, No. 2, 445–458. https://doi.org/10.2298/CSIS191229011D, (2020).
15. Wang D, Tan K, Li Z, et al. Research on Landmarks of SLAM Based on Square Root Cubature Kalman Filter. 3rd Annual International Conference on Information System and Artificial Intelligence (ISAI), 1037-1045. doi:10.1088/1742-6596/1069/1/012154,(2018).
16. Wang D, Tan K, Li H. Research on feature extraction method based on Simultaneous localization and mapping. China Control Conference (CCC), 3720-3724. doi:10.23919/ChiCC.2018.8482972,(2018).

17. Aydemir, F., Cetin, A. Point of Interest Coverage with Distributed Multi-Unmanned Aerial Vehicles on Dynamic Environment. Computer Science and Information Systems, Vol. 20, No. 3:1061–1084. https://doi.org/ 10.2298/CSIS221222037A,(2023).
18. Wang, Y., Han, D., Cui, M. Intrusion Detection Model of Internet of Things Based on Deep Learning. Computer Science and Information Systems, Vol. 20, No. 4. https://doi.org/10.2298/CSIS230418058W,(2023).
19. Zhang D , Shafiq M, Wang L,et al. Privacy-preserving remote sensing images recognition based on limited visual cryptography. CAAI Transactions on Intelligence Technology, Vol. 8, No. 4:1166-1177. https://doi.org/10.1049/cit2.12164,(2023).

Dandan Wang is a PhD candidate currently working at Huainan Normal University, with a main research focus on SINS and nonlinear filtering algorithms. Her five projects have received funding support from the provincial government, while her other projects have received funding support from other departments. She has published 10 SCI/EI papers and possesses rich teaching and strong research capabilities.

Zhaokun Zhu is a lecturer currently working at Zhengzhou Technology and Business University.His main research direction is electronic and communication engineering. In this article, he is mainly responsible for setting up the experimental environment.

Liang Yu is a lecturer currently working at Huainan Normal University, with a main research focus on mechanical design. One of his projects has received funding support from the provincial government and has been granted five patents. He has rich teaching experience.

Hongjie Li is a lecturer currently working at Anyang Institute of Technology. His main research direction is electronic technology, and he usually helps the college handle some academic affairs.

Kaituo Tan is a research assistant currently working at Huainan Normal University. His main research direction is automation technology. In this article, he is mainly responsible for experimental statistics and processing.

Received: April 18, 2024; Accepted: May 21, 2024.